

Chapter 9

Green Synthesis of Copper-Reinforced Cellulose Nanocomposites for Packaging Applications

P. Sivaranjana, E.R. Nagarajan, N. Rajini, A. Varada Rajulu and Suchart Siengchin

Abstract In the present work, cellulose nanocomposites dispersed with copper nanoparticles (CuNPs) were prepared using $\text{CuSO}_4 \cdot 5\text{H}_2\text{O}$ as the source and *Cassia alata* leaf extract as the reducing agent. These nanocomposites were prepared by regeneration method using ethanol as the coagulant. The morphology of generated CuNPs was viewed by SEM and TEM. The cellulose/CuNPs composite films showed good antibacterial activity against E-coil. The interaction between cellulose matrix and CuNPs was examined by FTIR and XRD. The changes in the thermal and tensile properties were examined with TGA and tensile tests. All these studies revealed that cellulose/CuNPs composites have enhanced thermal stability, tensile strength by the addition of CuNPs. These biodegradable cellulose/CuNPs composites films can be used for packaging and biomedical applications.

Keywords Biodegradable composites · CuNPs · *Cassia alata* leaves · Antibacterial activity

P. Sivaranjana · E.R. Nagarajan
Department of Chemistry, Kalasalingam University, Krishnankoil, Tamil Nadu 626126, India

N. Rajini
Department of Mechanical Engineering, Centre for Composite Materials, Kalasalingam University, Krishnankoil, Tamil Nadu 626126, India

N. Rajini (✉) · A.V. Rajulu
Centre for Composite Materials, International Research Center, Kalasalingam University, Krishnankoil, Tamil Nadu 626126, India
e-mail: rajiniklu@gmail.com

S. Siengchin
Graduate School of Engineering (TGS), King Mongkut's University of Technology North Bangkok, 1518 Wongsawang Road, Bangsue, Bangkok 10800, Thailand

9.1 Introduction

Nowadays, it is becoming very popular developing green composites, to minimize pollution, (Abdul Khalil et al. 2012). Various natural biodegradable fibres from different parts of the variety of plants were also used in this attempt. These natural fibres lack behind the synthetic fibres in terms of performance (Abdul Khalil et al. 2007), and so as to enhance the performance, several attempts of (Dufresne 2010; Chen et al. 2011; Deep et al. 2011) chemical modifications of natural fibres were done, which again eliminates wastes in another way. Bioreduction of metal nanoparticles was done by so many researchers using various plant extracts (Ahmed et al. 2016). In this study, methodology as well as the material used for developing the composites were also been checked for its environmental compatibility. The cellulose used as the matrix is an organic compound, highly crystalline, and can be made into transparent films, with high performance due to the presence of intermolecular hydrogen bonding. The performance of the composite is further enhanced by the addition of CuNPs as fillers into the cellulose matrix, which is synthesized by using the *Cassia alata* leaf extract as reducing agent, and copper sulphate pentahydrate as the source of metal particles. The raw materials used in this synthesis were eco-friendly, low cost, biodegradable, and process is also easy, economic, energy efficient and reproducible. Further, the reinforcement effect of Cu nanoparticle obtained from the leaf extract reducing agent is expected to produce good thermal stability, antibacterial activity and biodegradable.

9.2 Materials and Methods

9.2.1 Materials

In this present work, cotton linters (with a degree of polymerization Dp of 620) supplied by Hubei Chemical Fiber Co. Ltd. (Xiangfan, China) were used. LiOH, $\text{CuSO}_4 \cdot 5\text{H}_2\text{O}$ and Urea supplied by Hi Media laboratories pvt. Ltd (India) were used without purification. Ethyl alcohol was supplied by Ganesh Scientific (India). The *Cassia alata* leaves were collected locally and washed thoroughly with distilled water before preparing the extract.

9.2.2 *Cassia alata* Leaf Extraction

The *Cassia alata* leaves were collected, washed and cut into small pieces of even size. 10 wt% *Cassia alata* leaves by 10% the weight of distilled water maintained at 80 °C were taken and the mixture was kept for about 20 min. Then, the solution was cooled, filtered and the supernatant liquid was stored in the refrigerator.

9.2.3 Synthesis of Copper Nanoparticles

250 mM of aqueous copper sulphate solution was prepared using $\text{CuSO}_4 \cdot 5\text{H}_2\text{O}$ as the source. 10 ml of Cassia alata leaf extract was added to 100 ml of aqueous copper sulphate solution and kept under magnetic stirrer for uniform mixing for about 6 h. At once, the extract was introduced into the copper sulphate solution, and the colour of the solution changes gradually, indicating the reduction of copper to its nano form. The CuNPs formed were separated from the solution by repeated centrifugation at 12,000 rpm. Then, the CuNPs were washed repeatedly with distilled water and dried in hot air oven at 75 °C for about 2 h.

9.2.4 Dissolution of Cellulose

The aqueous solution of 8 wt% of LiOH and 15 wt% of urea was prepared and refrigerated to -12.5 °C, 4 wt% of cotton linters were added into the solution and stirred under mechanical stirrer and within 2 min the cellulose (cotton linters) got dissolved completely. The residues remaining undissolved were removed by centrifugation 7200 rpm at 5 °C. The clear stock solution was stored at 5 °C.

9.2.5 Preparation of Cellulose Wet Films with CuNPs

0.5, 1, 1.5, 2, 2.5 wt% of CuNPs were sonicated in 1 ml of water each to ensure uniform dispersion, and then it was added to the cellulose solutions under mechanical stirrer. The cellulose solutions with CuNPs were casted over glass plates and regenerated in alcohol bath for about 24 h, and then it was immersed in distilled water bath for about 3 h for the removal of alcohols and dissolved salts if any. Then, the films were dried over a smooth surface at room temperature.

9.2.6 FTIR Spectroscopic Analysis

The FTIR spectra of cellulose (matrix) and the composite films were recorded on a spectrum RXI Perkin Elmer FTIR spectrophotometer. All the spectra were recorded from 4000 to 500 cm^{-1} range with 45 scans in each case, at a resolution of 4 cm^{-1} .

9.2.7 Morphology

The presence of CuNPs in the nanocomposite films and the size distributions of CuNPs were examined by Carl Zeiss EVO 18 electron microscope. The copper element presence was confirmed by the EDX spectra using ESPIRIT software. The nanoparticles formed outside the film in solution were examined for their particle size distribution with Joel model JEM 210 transmission electron microscope.

9.2.8 Thermogravimetric Analysis

The primary and derivative thermograms of matrix and cellulose/CuNP composite films were recorded using TGA Q500 TA Instruments, USA, in the temperature range of 50–600 °C in nitrogen atmosphere at a heating rate of 10 °C/min.

9.2.9 Antibacterial Testing

200 ml of LB and agar containing medium was prepared and sterilized for 20 min, and the prepared medium was immediately transferred into sterile Petri plates. The plate was left for 15 min to solidify. After solidification, overnight cultured *E. coli* was taken in sterile buds and was swapped on the surface of the agar plates. Wells were punched on each plate using gel puncture. The circular discs of the matrix and the cellulose/CuNPs composite films with 0.5, 1, 1.5, 2, 2.5 wt% CuNPs were tested against pathogenic *E. coli* bacteria. The zones of clearance formed were recorded, and the diameter of zones was measured.

9.3 Result and Discussion

9.3.1 Appearance of Matrix and Cellulose/CuNPs Composite Film

In order to examine the effect of CuNPs on the appearance of the nanocomposite films prepared, the photographs of the matrix and the nanocomposites prepared using 0.5, 1, 1.5, 2, 2.5 wt% of CuNPs using aqueous $\text{CuSO}_4 \cdot 5\text{H}_2\text{O}$ solution as the source for CuNPs were regarded and are presented in Fig. 9.1.

From Fig. 9.1, it is evident the matrix and composite films were transparent, and with increase in the wt% of CuNPs the colour becomes brownish, but the intensity

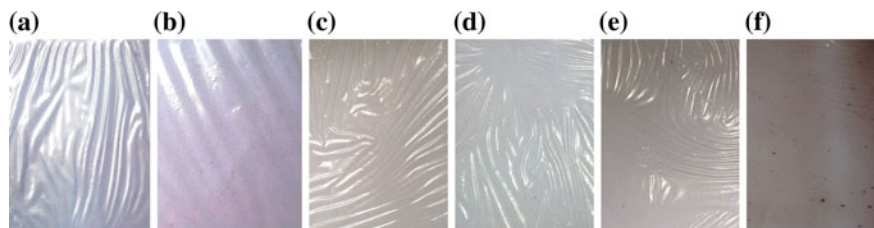


Fig. 9.1 Photographs of matrix and cellulose/CuNP composite films

of the colour was not uniform, even brown spots are viewed at higher concentration of 2.5 wt% of CuNPs due to the agglomeration of nanoparticles, as its concentration increases. Whereas in the case of newly generated systems, the intensity of colour change was uniform (Sadanand et al. 2016), indicating the even distribution of nanoparticles inside the film.

9.3.2 Size of the CuNPs Formed by Using the Cassia alata Leaf Extract as Reducing Agent

The CuNPs formed were separated by series of centrifugation and dried. To examine the nature of CuNPs formed, the TEM and SEM micrographs were recorded and are presented in Fig. 9.2. Using SEM micrograph, the particle size of one hundred CuNPs was measured and the particle size distribution is also presented in the same Fig. 9.2. The EDX spectrum of the particles is also presented in Fig. 9.2.

From Fig. 9.2, it is evident that the CuNPs formed were spherical in nature, and further the average size of one hundred particles selected was 71 nm. The presence of CuNPs was confirmed by EDX spectrum. Further, most of the CuNPs produced have the size in the 60–69 nm range.

9.3.3 Distribution of Ex situ Generated CuNPs Inside the Matrix

The distribution of ex situ generated CuNPs inside the cellulose/CuNPs composite films was recorded as an example; the fractographs of the composite films prepared with 0.5–2.5 wt% CuNPs are presented in Fig. 9.3. From fig (a) and (b), it is evident that as the concentration of CuNPs increases the agglomeration occurs. The corresponding EDX spectra are also presented in Fig. 9.3c and d which confirms the presence of CuNPs inside the composite films.

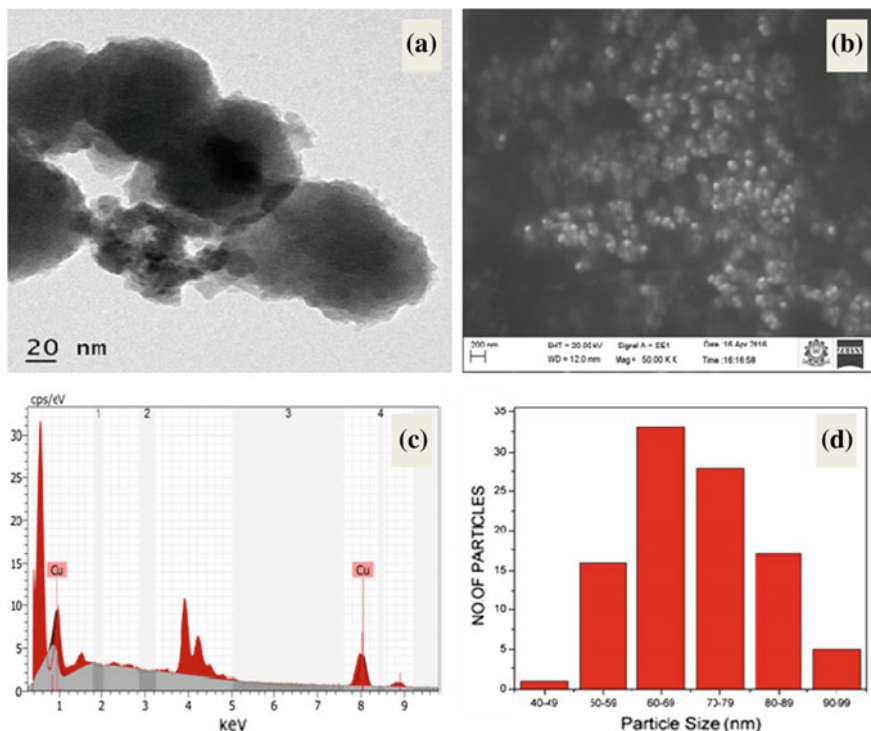


Fig. 9.2 a and b TEM and SEM image of CuNPs, c EDX of reduced CuNPs, d particle size distribution of reduced CuNPs

9.3.4 Interaction Between Matrix and CuNPs

In order to prove the interactions between matrix and CuNPs, the FTIR spectra of the matrix and the composites were regarded and are presented in Fig. 9.4.

From Fig. 9.4, it is evident that the spectrum of matrix is similar to that of the composites except, an increase in the intensity of all the bands in the case of the composites. It implies that the dispersed CuNPs did not change the chemical structure of cellulose matrix (Tsurumi et al. 1990) and were held within the cellulose matrix by electrostatic forces.

The common bands observed at 3344 cm^{-1} belong to $-\text{OH}$ group of the cellulose; the other band 2901 and 1021 cm^{-1} was due to the vibrations of $-\text{CH}_2$ and $-\text{C}-\text{OH}$ groups of cellulose. The peak observed at 1651 cm^{-1} was due to crystallization of water.

The bands observed at 1424 and 1365 cm^{-1} were due to $\text{C}-\text{CH}$ asymmetric deformation and $\text{C}-\text{CH}$ scissoring modes of cellulose. The other bands obtained at 1260 and 1158 cm^{-1} were due to the $-\text{COO}$ vibration of acetyl groups present in hemicelluloses and antisymmetric bridge stretching vibrations of cellulose in the

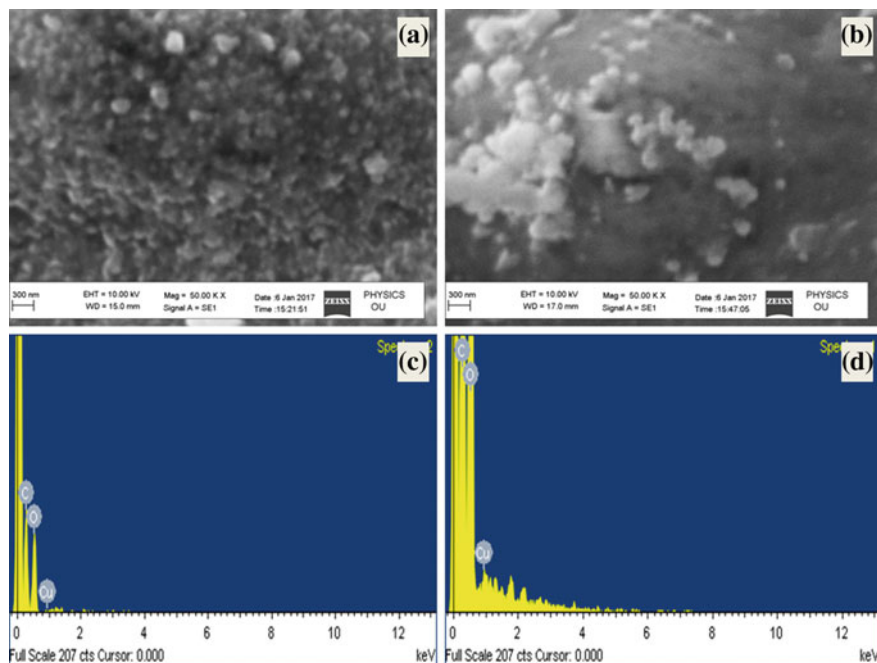


Fig. 9.3 a and b SEM images of composite films with 5 and 2.5 wt% of CuNPs, c and d EDX spectra of composite films with 5 and 2.5 wt% of CuNPs

leaf extract. Further, the bands at 895 , 710 and 677 cm^{-1} were due to $=\text{C}-\text{H}$ stretching and bending in cellulose.

9.3.5 Antibacterial Activity

As CuNPs possess antibacterial activity, the antibacterial activity of cellulose nanocomposite films with dispersed CuNPs was examined. For this, the antibacterial activity test was conducted against *E.coli* bacteria, by disc method. The clear zones observed for the matrix, and composites were photographed and are presented in Fig. 9.5. In each case, the diameter of clear zone was measured and shown in Fig. 9.5.

From Fig. 9.5, it is evident that the matrix does not show any antibacterial activity against *E. coli* bacteria, whereas on increase in the wt% of CuNPs in the cellulose/CuNPs composites films the antibacterial activity against *E. coli* bacteria increases.

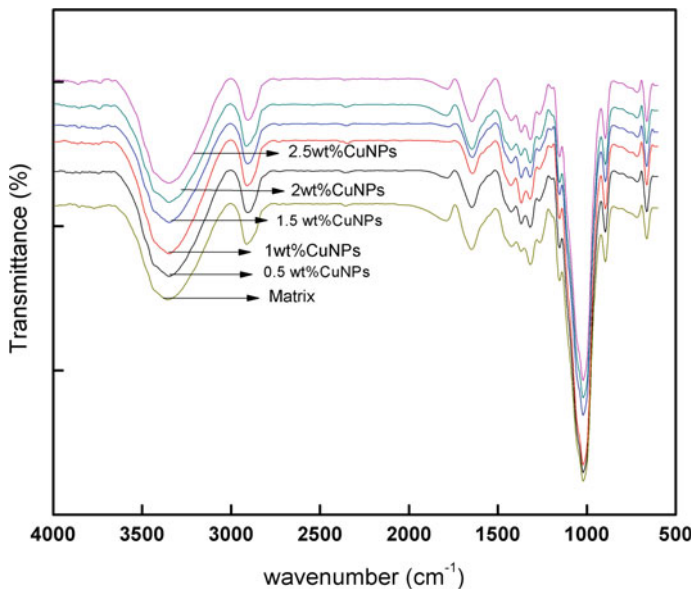


Fig. 9.4 FTIR spectra of matrix and cellulose/CuNPs composites

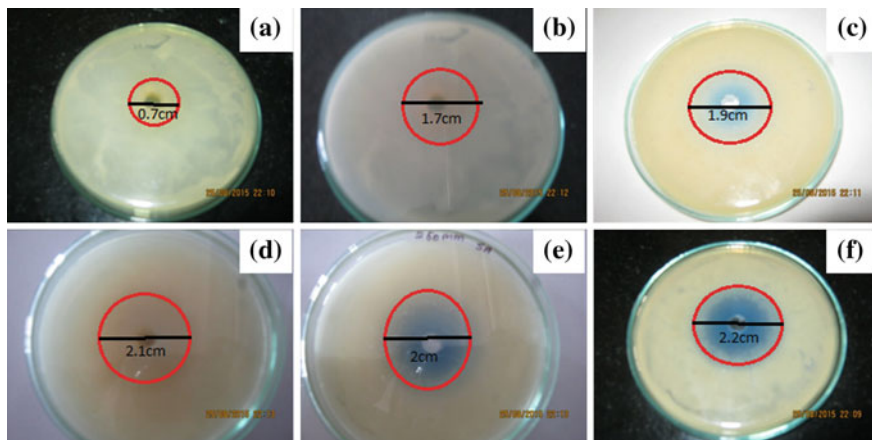


Fig. 9.5 a Antibacterial activity of matrix cellulose, b cellulose/0.5% CuNPs composites, c cellulose/1% CuNPs composites, d cellulose/1.5% CuNPs composites, e cellulose/2% CuNPs composites, f cellulose/2.5% CuNPs composites

9.3.6 X-Ray Diffraction Analysis

In order to study the effect of dispersed CuNPs on the crystallinity nanocomposite films, the X-ray diffractograms of matrix and cellulose/CuNPs composites dispersed with different wt% of CuNPs were recorded and are presented in Fig. 9.6.

From Fig. 9.6, it is evident that there are two main peaks similar in the case of matrix and the composite $2\theta = 12.8^\circ$ and 21.9° corresponding to reflections from (1–10) to (200) planes of cellulose II (Zhang et al. 2001). On close examination of the diffractogram corresponding to the composites made with different wt% of CuNPs, some additional peaks were observed at $2\theta = 23.3, 32.3, 33.1, 35.6, 38.4, 46.5, 54.6$ and 57.9 , which are comparable to JCPDS standards of CuO particles (Kulkarni et al. 2015); further, the peaks at 39.7 and 68.7 correspond to the cubic-centred CuNPs (Alekseeva et al. 2011). Of these, the peaks observed at 32.3° and 36.8° were assigned to Cu_2O nanoparticles arising from diffractions from (002) and (111) planes respectively whereas the other two peaks at 43.9° and 50.8° were assigned to CuNPs resulting from the diffractions by (111) and (200) planes respectively. Similar observation was made by Sadanand et al. (2016) in case of cellulose/CuNP composite films reduced by ocimum sanctum leaf extract. X-ray diffractograms of the composites clearly indicate the presence of the both CuNPs and Cu_2NPs as a mixture.

The broadening of the XRD peaks in the cellulose/CuNPs composites indicates the decrease in the crystallinity of the cellulose by the filling up of biointerfaces by CuNPs.

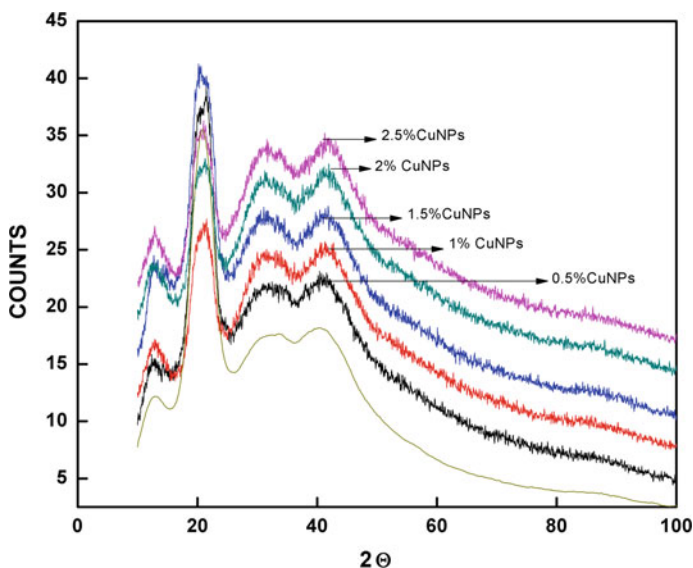


Fig. 9.6 X-ray diffractograms of matrix and cellulose/CuNPs composites

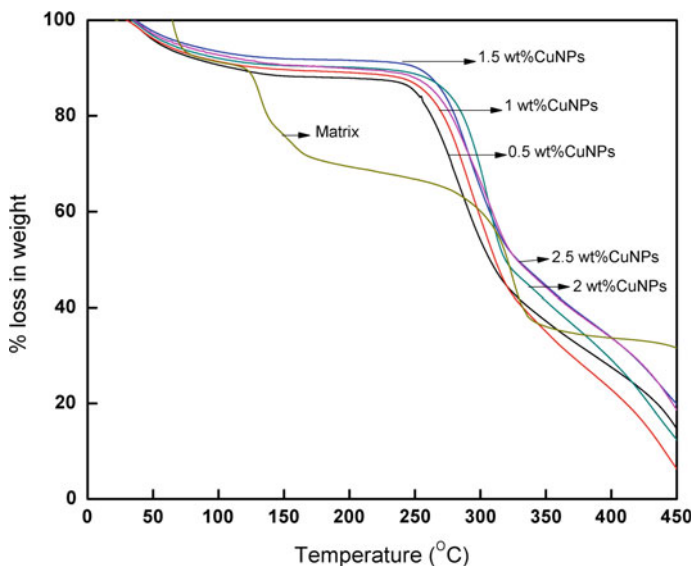


Fig. 9.7 Primary thermogram of matrix and cellulose/CuNPs composites

9.3.7 Thermal Properties

To investigate the effect of CuNPs on the thermal stability of the composites, the authors carried the thermogravimetric analysis of the matrix and the composites. The primary thermogram for the matrix and composites with different wt% of CuNPs are presented in Fig. 9.7. The thermal stability of the composites was greater than the matrix due to the addition of CuNPs which prolonged the degradation process.

9.4 Conclusions

The cellulose-based CuNPs-reinforced composite films were synthesized using *Cassia alata* leaf extract as reducing agent to enhance the properties of cellulose film. The nanolevel particles size range of 60–69 nm was noticed with the aid of transmission electron microscope and scanning electron microscope. A significant improvement in the increase of crystallinity was observed in the newly generated CuNPs-reinforced composite films. The enhanced thermal stability of around 57% of increase was found in the case particle-reinforced films compared to the pure matrix. However, no liner trend in the increase of thermal stability of the nanocomposites was observed with increasing CuNPs content. Regarding to the antibacterial activity, the increase in particle content exhibits gradual improvement

in resistance property. Among various concentrations, the 2.5 wt% Cu showed maximum antibacterial activity of 68% improvement which could be the good sign to propose this material to microbial applications. Based on the thermal stability and the antibacterial activity, the cellulose/CuNPs composites can be considered for usage in packaging and biomedical applications.

References

- Abdul Khalil HPS, Hanida S, Kang CW, Nik Fuaad NA (2007) Agro-hybrid composite: the effects on mechanical and physical properties of oil palm fiber (EFB)/glass hybrid reinforced polyester composites. *J Reinf Plast Compos* 26:203–218
- Abdul Khalil HPS, Bhat AH, Yusra AFI (2012) Green composites from sustainable cellulose nanofibrils: a review. *Carbohyd Polym* 87(2012):963–979
- Ahmed Shakeel, Ahmad Mudasar, Swami Babu Lal, Ikram Saiqa (2016) A review on plants extract mediated synthesis of silver nanoparticles for antimicrobial applications: a green expertise. *J Adv Res* 7:17–28
- Alekseeva O, Chulovskaya S, Bagrovskaya N (2011) Copper nanoparticle composites based on cellulose derivatives. *Chem Chem Technol* 5:447–450
- Chen WY, Liu H, Chen Y, Zhang P, Hai M, Parfenyuk YV (2011) Individualization of cellulose nanofibers from wood using high-intensity ultrasonication combined with chemical pretreatments. *Carbohyd Polym* 83:1804–1811
- Deepa B, Abraham E, Cherian BM, Bismarck A, Blaker JJ, Pothan LA, Leao AL, de Souza SF, Kottaisamy M (2011) Structure, morphology and thermal characteristics of banana nano fibers obtained by steam explosion. *Biores Technol* 102:1988–1997
- Dufresne A (2010) Processing of polymer nanocomposites reinforced with polysaccharide nanocrystals. *Molecules* 15(6):4111–4128
- Kulkarni V, Suryawanshi S, Kulkarni P (2015) Biosynthesis of copper nanoparticles using aqueous extract of Eucalyptus sp. plant leaves. *Curr Sci* 109(2):25
- Sadanand V, Rajini N, Satyanarayana B, Varada Rajulu A (2016) Preparation of cellulose composites with in situ generated copper nanoparticles using leaf extract and their properties. *Carbohyd Polym* 150:32–39
- Tsurumi T, Osawa N, Hitaka H, Hirasaki T, Yamaguchi K, Manabe S, Yamashiki T (1990) Structure of cuprammonium regenerated cellulose hollow fiber (BMM Hollow fiber) for virus removal. *Polym J* 22(8):751–758
- Zhang L, Ruan D, Zhoul J (2001) Structure and properties of regenerated cellulose films prepared from cotton linters in NaOH/Urea aqueous solution. *Ind Eng Chem Res* 40:5923–5928